Eur. Phys. J. B **5**, 187–192 (1998)

THE EUROPEAN PHYSICAL JOURNAL B

Investigations on phase locking in a two-dimensional Josephson junction array within the Werthamer and the RCSJ model

B. Frank[a], K.Yu. Platov[b], and W. Krech[c]

Friedrich-Schiller-Universität Jena, Institut für Festkörperphysik, Max-Wien-Platz 1, 07743 Jena, Germany

Received: 23 March 1998 / Revised: 3 June 1998 / Accepted: 9 June 1998

Abstract. The synchronization properties of a simple two-dimensional Josephson array consisting of two coupled SQUID cells are studied within the Werthamer as well as the RCSJ model. Special emphasis is placed on the role of inductances arranged perpendicular and parallel to the current bias direction for the phase locking behavior. The general behavior within the Werthamer model is found to be similar to that within the RCSJ model. However, there are quantitative differences, *e.g.* an enhanced phase shift between the voltage oscillations within one cell and a shift of the parameter range for the in-phase regime between different cells towards lower values of the McCumber parameter in the Werthamer model.

PACS. 74.50.+r Proximity effects, weak links, tunneling phenomena, and Josephson effects

1 Introduction

Two-dimensional Josephson junction arrays have been under consideration as tunable microwave oscillators providing a high radiation output [1,2]. Therefore, there is a great interest on understanding the phase locking behavior of such arrays. Up to now, theoretical investigations [3–9] are based on the RCSJ (resistively and capacitively shunted junction) model [10,11] which describes the behavior of shunted tunnel junctions well. Nethertheless, arrays consisting of unshunted small-area Josephson tunnel junctions with high current densities are also conceivable [12–14]. They allow the preparation of more compact arrays with small loop inductances; problems connected with the parasitic shunt impedance could be avoided. For this kind of junctions the Werthamer theory [15] supplies a more appropriate description. In this paper we study synchronization properties of a basic two-dimensional array in the Werthamer as the well as the RCSJ model. Our aim is to decide to what extend results obtained in the more simple RCSJ model are valid for arrays consisting of unshunted tunnel junctions, too. Supplementing to recent theoretical papers [16,17] we treat the array shown in Figure 1 where a special emphasis is taken on the role of inductances arranged perpendicular and parallel to the current bias direction for the phase locking behavior. In Section 2 we write down the basic dynamic equations of the array within the Werthamer and the RCSJ model. In Section 3 an analytical treatment is given within the RCSJ model. Finally, in Section 4 we present numerical results for both models.

[a] e-mail: p5bifr@rz.uni-jena.de
[b] e-mail: okp@rz.uni-jena.de
[c] e-mail: owk@rz.uni-jena.de

2 Werthamer and RCSJ model

Within the Werthamer model the dynamics of a Josephson tunnel junction is described by a normalized integro-differential equation for the Josephson phase ϕ [15]

$$\beta_c\ddot{\phi}(s) + \dot{\phi}(s) + i_w(s) = i_0 \tag{1}$$

with

$$i_w(s) = -\int_{-\infty}^{s} ds' \Bigg\{ p(s-s') \sin\left[\frac{1}{2}\left(\phi(s') + \phi(s)\right)\right] + q^0(s-s') \sin\left[\frac{1}{2}\left(\phi(s') - \phi(s)\right)\right] \Bigg\} . \tag{2}$$

Here we introduced the quantities

$$s = \frac{2eR_N I_C}{\hbar} t, \qquad \beta_C = \frac{2e}{\hbar} I_C R_N^2 C, \qquad i_0 = \frac{I_0}{I_C}; \tag{3}$$

β_C is the McCumber parameter, $I_C = I_C(T)$ denotes the critical current and I_0 the bias current; R_N is the normal-state resistance, C is the capacitance of the junction. The dot ($\dot{}$) means the derivative with respect to the dimensionless time s. The normalized voltage $v = V/I_C R_N$ across the tunnel junction is related to the Josephson phase difference ϕ by $v = \dot{\phi}$. The response functions $p(s)$ and $q^0(s)$ can be described realistically, *e.g.* within the so-called

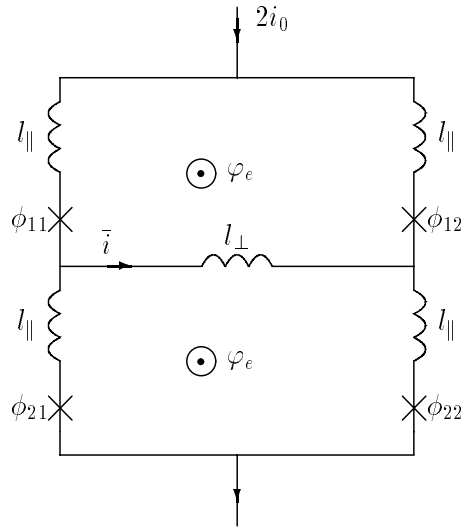

Fig. 1. The simple two-dimensional Josephson junction array under consideration.

smeared BCS model [18–20] with a complex superconducting gap parameter $\Delta(1 - i\eta)$. For our numerical calculations we exploited the method of Odintsov *et al.* [21] which approximates the kernels $p(s)$ and $q^0(s)$ for $\eta = 0.02$ and $T = 0.6T_C$ by respective sums of exponential functions, *cf.* [22].

Note that after setting $p(s) = -\delta(s)$ (here $\delta(s)$ is the Dirac delta function) and $q^0(s) = 0$, the time retardation of the Werthamer integral (2) is lost. We get

$$i_w(s) = \sin\phi \tag{4}$$

leading to the RCSJ differential equation

$$\beta_c\ddot{\phi}(s) + \dot{\phi}(s) + \sin\phi(s) = i_0. \tag{5}$$

Applying equations (1) to the circuit shown in Figure 1, the following set of equations can be derived

$$\beta_c\ddot{\phi}_{kl} + \dot{\phi}_{kl} + i_w(\phi_{kl}) = i_{kl}\ , \quad k,l = 1,2, \tag{6}$$

$$\phi_{k2} - \phi_{k1} - \varphi_e + (-1)^k l_\perp\bar{i} + (i_{k2} - i_{k1})l_\parallel = 0, \quad k = 1,2 \tag{7}$$

and

$$2i_0 = i_{11} + i_{12} = i_{21} + i_{22}, \tag{8}$$

$$\bar{i} = i_{11} - i_{21} = i_{22} - i_{12}. \tag{9}$$

Equation (7) arises from the flux quantization around the boundaries of both cells where the mutual inductance terms have been neglected. The parameters

$$l_{\perp,\parallel} = 2\pi I_C L_{\perp,\parallel}/\Phi_0 \tag{10}$$

describe the normalized inductances arranged perpendicular and parallel to the current bias direction (*cf.* Fig. 1) and φ_e means the normalized external flux $\varphi_e = 2\pi\Phi_e/\Phi_0$. ($\Phi_0$ is the flux quantum.)

3 Analytical treatment within the RCSJ model

In frame of the RCSJ model the array shown in Figure 1 can be treated analytically by means of a harmonic expansion procedure. As we will see in Section 4, the analytical results allow to understand our numerical calculations within the RCSJ as well as within the rather complicated Werthamer model.

In case of the RCSJ model equations (7, 9) will be simplified by setting $i_w(s) = \sin\phi$, *cf.* equation (4). Following the treatment of Basler *et al.* (see [16,23] for a more detailed description of this method), we introduce sum and difference variables

$$\Sigma_k = \frac{1}{2}(\phi_{k2} + \phi_{k1}), \tag{11}$$

$$\Delta_k = \frac{1}{2}(\phi_{k2} - \phi_{k1}) \tag{12}$$

and define the rescaled variables

$$\tilde{\beta}_c = i_0\beta_c, \ \ \tilde{l}_{\perp,\parallel} = i_0 l_{\perp,\parallel}, \ \ \tilde{s} = i_0 s. \tag{13}$$

The corresponding time derivation with respect to $\tilde{s}$ will be denoted by a dash. The resulting equations

$$\tilde{\beta}_c\Delta_k'' + \Delta_k' + b\cos\Sigma_k\sin\Delta_k = -(-1)^k\frac{1}{2(\tilde{l}_\perp + \tilde{l}_\parallel)}(\Delta_2 - \Delta_1) + \frac{1}{2\tilde{l}_\parallel}(\varphi_e - \Delta_1 - \Delta_2), \tag{14}$$

$$\tilde{\beta}_c\Sigma_k'' + \Sigma_k' + b\sin\Sigma_k\cos\Delta_k = 1 \tag{15}$$

can be solved by means of a harmonic expansion concerning the parameter $b = i_0^{-1}$. In a straightforward procedure we find the solutions up to the first order

$$\Sigma_k = \Sigma_k^0 + b\Sigma_k^1, \tag{16}$$

$$\Delta_k = \Delta_k^0 + b\Delta_k^1, \tag{17}$$

where

$$\Sigma_k^0 = \tilde{s} + \delta_k + \pi/2, \tag{18}$$

$$\Delta_k^0 = \frac{\varphi_e}{2}, \tag{19}$$

$$\Sigma_k^1 = \frac{\cos\dfrac{\varphi_e}{2}}{1 + \tilde{\beta}_c^2}\left[\ \tilde{\beta}_c\cos(\tilde{s} + \delta_k) - \sin(\tilde{s} + \delta_k)\ \right], \tag{20}$$

$$\Delta_k^1 = S(\tilde{s}) - (-1)^k D(\tilde{s}) \tag{21}$$

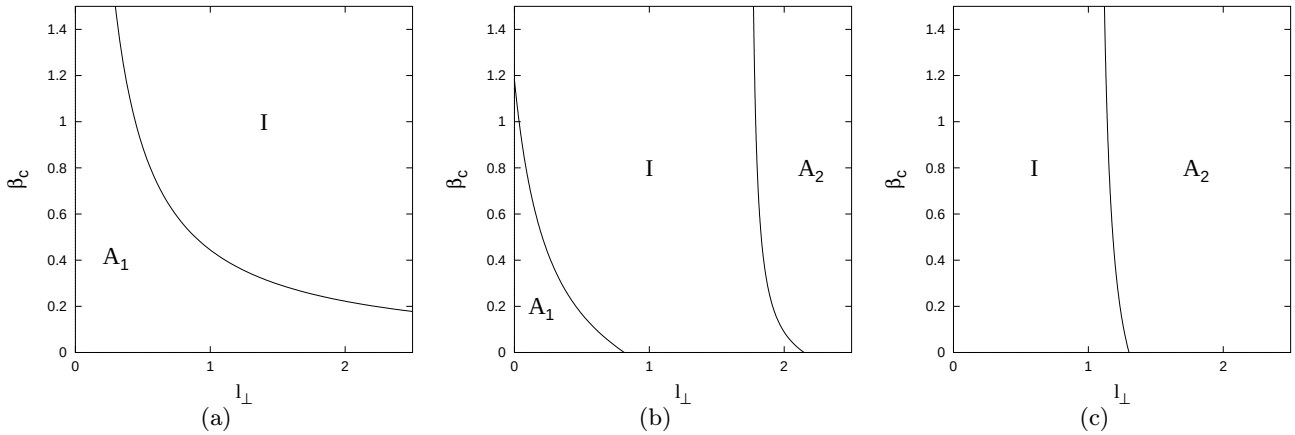

Fig. 2. Transition between the in-phase (I) and antiphase (A_1, A_2) regions of the voltage oscillations in the two cells obtained from the analytical approximation within the RCSJ model for $i_0 = 1.5$ and (a) $l_\parallel = 0$, (b) $l_\parallel = 0.3$ and (c) $l_\parallel = 0.7$. With increasing $l_\parallel$ the boundary lines move to lower values of β_c; the lower boundary line vanishes for $l_\parallel > 1/i_0$.

with the abbreviations

$$D(\tilde{s}) = \frac{\sin\frac{\varphi_e}{2}}{1+\left(\tilde{\beta}_c - \frac{1}{\tilde{l}_\parallel + \tilde{l}_\perp}\right)^2} \sin\frac{\delta_1-\delta_2}{2}$$

$$\times \left[\sin\left(\tilde{s}+\frac{\delta_1+\delta_2}{2}\right) - \left(\tilde{\beta}_c - \frac{1}{\tilde{l}_\parallel+\tilde{l}_\perp}\right)\cos\left(\tilde{s}+\frac{\delta_1+\delta_2}{2}\right)\right],$$

$$S(\tilde{s}) = -\frac{\sin\frac{\varphi_e}{2}}{1+\left(\tilde{\beta}_c - \frac{1}{\tilde{l}_\parallel}\right)^2} \cos\frac{\delta_1-\delta_2}{2}$$

$$\times \left[\cos\left(\tilde{s}+\frac{\delta_1+\delta_2}{2}\right) + \left(\tilde{\beta}_c - \frac{1}{\tilde{l}_\parallel}\right)\sin\left(\tilde{s}+\frac{\delta_1+\delta_2}{2}\right)\right].$$

In the focus of our interest are on the one hand the phase differences ϑ_k of the oscillations within the kth cell but on the other hand the shift between the respective phases of different cells. For the determination of the last one we use the well-known phase-slip method [24], assuming only slowly varying phases

$$\delta_k = \delta_k(\tilde{s}), \quad |\,\delta_k'\,| \ll 1. \tag{22}$$

Inserting equations (19, 21) in equation (15) and averaging over the Josephson oscillation period, we obtain a differential equation for the mean phase shift $\delta = \langle\delta_1\rangle - \langle\delta_2\rangle$

$$\beta_c\delta'' + \delta' = \frac{b^2}{2}\sin^2\frac{\varphi_e}{2}$$

$$\times \left\{ \frac{\frac{1}{\tilde{l}_\perp+\tilde{l}_\parallel} - \tilde{\beta}_c}{1+\left[\frac{1}{\tilde{l}_\perp+\tilde{l}_\parallel} - \tilde{\beta}_c\right]^2} - \frac{\frac{1}{\tilde{l}_\parallel} - \tilde{\beta}_c}{1+\left[\frac{1}{\tilde{l}_\parallel} - \tilde{\beta}_c\right]^2}\right\} \sin\delta. \tag{23}$$

From equation (23) we find two kinds of phase locking solutions, corresponding to the antiphase ($\delta^{lock} = \pi$) and in-phase ($\delta^{lock} = 0$) type, respectively. Assuming a small perturbation of the locking solution $\delta(\tilde{s}) = \delta^{lock} + \epsilon\exp\lambda\tilde{s}$, we can derive the stability condition

$$\left\{ \frac{\frac{1}{\tilde{l}_\perp+\tilde{l}_\parallel} - \tilde{\beta}_c}{1+\left[\frac{1}{\tilde{l}_\perp+\tilde{l}_\parallel} - \tilde{\beta}_c\right]^2} - \frac{\frac{1}{\tilde{l}_\parallel} - \tilde{\beta}_c}{1+\left[\frac{1}{\tilde{l}_\parallel} - \tilde{\beta}_c\right]^2}\right\}$$

$$\times \sin^2\frac{\varphi_e}{2}\cos\delta^{lock} < 0\,, \tag{24}$$

stipulating the boundaries between the parameter regions corresponding to the in-phase or antiphase regime for finite values of external flux ($\varphi \neq 2n\pi$). In the limit $l_\parallel \to 0$ the simple curve $\tilde{\beta}_c = 1/\tilde{l}_\perp$ [16] separates in-phase and antiphase solutions whereas for finite values $l_{\perp,\parallel}$ the stable in-phase regime is restricted by an upper and a lower boundary given by

$$\frac{1}{\tilde{l}_\parallel} + \frac{1}{\tilde{l}_\parallel+\tilde{l}_\perp} - \sqrt{\left(\frac{1}{\tilde{l}_\parallel} - \frac{1}{\tilde{l}_\parallel+\tilde{l}_\perp}\right)^2 + 1} < \tilde{\beta}_c$$

$$< \frac{1}{\tilde{l}_\parallel} + \frac{1}{\tilde{l}_\parallel+\tilde{l}_\perp} + \sqrt{\left(\frac{1}{\tilde{l}_\parallel} - \frac{1}{\tilde{l}_\parallel+\tilde{l}_\perp}\right)^2 + 1} \tag{25}$$

as shown in Figure 2.

With increasing values of the inductivities parallel to the current bias direction ($l_\parallel$) the lower antiphase region A_1 shrinks in favour of the in-phase regime. On the other hand, a second antiphase region A_2 appears, however, it plays no role in parameter regions of practical interest ($\beta_c,\ l_{\perp,\parallel} < 1$).

Note that in the zero-field limit the stability regime is undetermined as discussed by Filatrella and Wiesenfeld *et al.* [3,4].

Now we discuss the next question concerning the phase difference ϑ_k between the voltages in the same cell. We restrict us to the first cell. The corresponding voltage oscillations can be obtained differentiating the Josephson phases

$$\phi_{1l} = \Sigma_1 + (-1)^l \Delta_1, \quad l = 1, 2 \tag{26}$$

and using the solutions (16)-(21) for Σ_1 and Δ_1. From the resulting voltages

$$\begin{aligned} v_{1l} &= \dot{\phi_{1l}} \\ &= i_0 - \frac{\cos\frac{\varphi_e}{2}}{1+\tilde{\beta}_c^2} \left[\tilde{\beta}_c \sin(\tilde{s}+\delta_1) + \cos(\tilde{s}+\delta_1) \right] \\ &\quad + (-1)^l \left[\dot{S}(\tilde{s}) + \dot{D}(\tilde{s}) \right] \\ &= i_0 + a_l \cos\tilde{s} + b_l \sin\tilde{s} \end{aligned} \tag{27}$$

we can read out the first order Fourier coefficients

$$\begin{aligned} a_l &= -\frac{\cos\frac{\varphi_e}{2}}{1+\tilde{\beta}_c^2} \left[\tilde{\beta}_c \sin\delta + \cos\delta \right] \\ &\quad + (-1)^l \frac{1}{2} \frac{\sin\frac{\varphi_e}{2}}{1+\left(\tilde{\beta}_c - \frac{1}{\tilde{l}_\parallel}\right)^2} \\ &\quad \times \left[\sin\delta - \left(\tilde{\beta}_c - \frac{1}{\tilde{l}_\parallel}\right)\left(1+\cos\delta\right) \right] \\ &\quad + (-1)^l \frac{1}{2} \frac{\sin\frac{\varphi_e}{2}}{1+\left(\tilde{\beta}_c - \frac{1}{\tilde{l}_\parallel + \tilde{l}_\perp}\right)^2} \\ &\quad \times \left[\sin\delta + \left(\tilde{\beta}_c - \frac{1}{\tilde{l}_\parallel + \tilde{l}_\perp}\right)\left(1-\cos\delta\right) \right], \end{aligned} \tag{28}$$

$$\begin{aligned} b_l &= \frac{\cos\frac{\varphi_e}{2}}{1+\tilde{\beta}_c^2} \left[-\tilde{\beta}_c \cos\delta + \sin\delta \right] \\ &\quad + (-1)^l \frac{1}{2} \frac{\sin\frac{\varphi_e}{2}}{1+\left(\tilde{\beta}_c - \frac{1}{\tilde{l}_\parallel}\right)^2} \left[\left(\tilde{\beta}_c - \frac{1}{\tilde{l}_\parallel}\right)\sin\delta + 1 + \cos\delta \right] \\ &\quad + (-1)^l \frac{1}{2} \frac{\sin\frac{\varphi_e}{2}}{1+\left(\tilde{\beta}_c - \frac{1}{\tilde{l}_\parallel + \tilde{l}_\perp}\right)^2} \left[\left(\tilde{\beta}_c - \frac{1}{\tilde{l}_\parallel + \tilde{l}_\perp}\right) \right. \\ &\quad \left. \times \sin\delta + \cos\delta - 1 \right]. \end{aligned} \tag{29}$$

Here, without lack of generality we have set $\delta_2 = 0$ and hence $\delta_1 = \delta$. Then, the in-phase regime between the cells corresponds to $\delta = 0$, the antiphase regime to $\delta = \pi$. Considering only these relevant cases we get the more simple expressions

$$\begin{aligned} (a_l)_{I,A} &= \pm \left\{ -\frac{\cos\frac{\varphi_e}{2}}{1+\tilde{\beta}_c^2} + (-1)^l \right. \\ &\quad \left. \times \frac{\sin\frac{\varphi_e}{2}}{1+\left(\tilde{\beta}_c - \frac{1}{\tilde{l}_{I,A}}\right)^2} \left(\frac{1}{\tilde{l}_{I,A}} - \tilde{\beta}_c\right) \right\}, \end{aligned} \tag{30}$$

$$\begin{aligned} (b_l)_{I,A} &= \pm \left\{ -\frac{\cos\frac{\varphi_e}{2}}{1+\tilde{\beta}_c^2}\tilde{\beta}_c + (-1)^l \right. \\ &\quad \left. \times \frac{\sin\frac{\varphi_e}{2}}{1+\left(\tilde{\beta}_c - \frac{1}{\tilde{l}_{I,A}}\right)^2} \right\}. \end{aligned} \tag{31}$$

The parameters $\tilde{l}_{I,A}$ characterize the inductances which cause the phase shift in the in-phase or antiphase regime, respectively:

$$\begin{aligned} \tilde{l}_I &= \tilde{l}_\parallel, \\ \tilde{l}_A &= \tilde{l}_\perp + \tilde{l}_\parallel. \end{aligned} \tag{32}$$

The plus sign in equations (30, 31) belongs to the in-phase (I) and the minus sign to the antiphase (A) solution. Note that this sign distinction is of no importance for the phase difference $\vartheta \equiv \vartheta_1$ within the first cell which can be determined from

$$\vartheta = \begin{cases} \bar{\vartheta} & \text{for} \quad a_1 b_2 \geq b_1 a_2, \\ 2\pi - \bar{\vartheta} & \text{for} \quad a_1 b_2 < b_1 a_2, \end{cases} \tag{33}$$

where

$$\bar{\vartheta} = \arccos \frac{a_1 a_2 + b_1 b_2}{\sqrt{(a_1^2 + a_2^2)(b_1^2 + b_2^2)}}.$$

The internal phase shift ϑ as function of external flux according to equation (33) is shown in Figure 3 for some instructive parameters. Compared with the results of the single SQUID cell [25] the behavior is more complicated. We have to take into account the specific role of the inductances perpendicular and parallel to the current bias direction and to distinguish between the in-phase and antiphase regime between the cells. The value of the inductance $l_\perp$ can not influence ϑ in the in-phase regime. Hence, for a vanishing parallel inductance $l_\parallel$ we find no phase shift ϑ. This is caused by the fact that only in the antiphase regime an ac current flows through the inductance $l_\perp$. Nethertheless, the value of $l_\perp$ can determine wether the in-phase or the antiphase regime is realized. This is illustrated in Figure 3c. Here $l_\perp$ is chosen large enough to achieve an in-phase regime between the cells (*cf.* Fig. 2a) but in the in-phase branch it causes no phase shift.

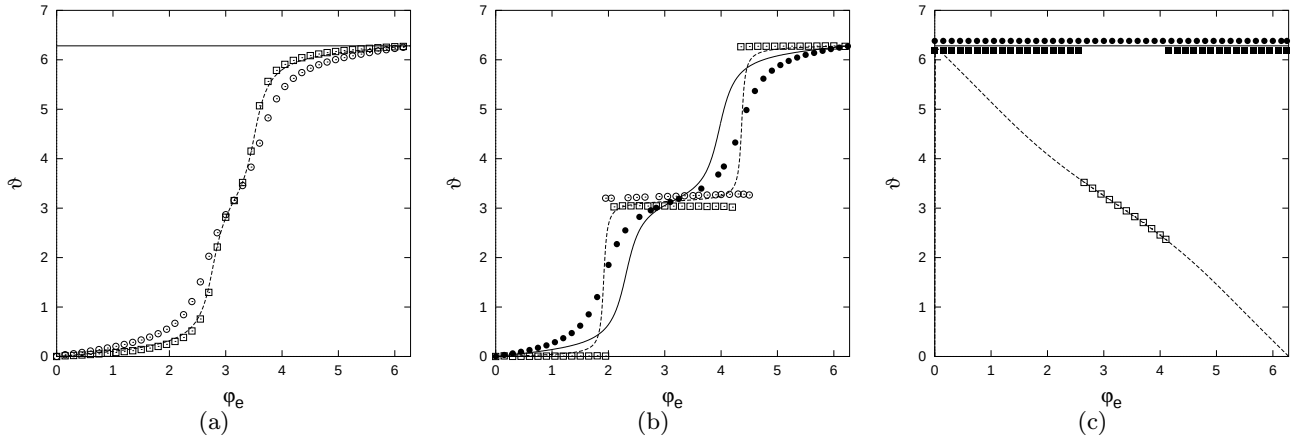

Fig. 3. Phase shift ϑ of the voltage oscillations within the first cell. The possible branches for the in-phase (solid line) and antiphase (dashed line) regime are obtained from the analytical approximation within the RCSJ model. The numerical results within the RCSJ (boxes) and the Werthamer (circles) model are indicated by open (antiphase regime) or filled (in-phase regime) symbols; the parameters are $i_0 = 1.5$, $\beta_c = 0.5$ and (a) $l_\perp = 0.1$, $l_\parallel = 0$, (b) $l_\perp = 0.1$, $l_\parallel = 0.2$, (c) $l_\perp = 1.4$, $l_\parallel = 0$.

4 Numerical simulation within the Werthamer and RCSJ model

In this section we will confirm our analytical approximations within the RCSJ model by numerical simulations and extend our investigations to the Werthamer model. For this purpose we have to solve equations (6-9) combined with (2) or (4), respectively. In Figure 4 the numerically calculated lower boundary between the in-phase (I) and antiphase (A_1) regime is shown. For the simulations an external flux $\varphi_e = 1$ is used because in the zero-field limit the locking regime is undetermined (according to Eq. (24)). Within the RCSJ model the comparison with the analytical curves shows a good agreement, at least for larger McCumber parameters $\beta_c > 0.6$; the quantitative deviations for small values of β_c are caused by the increasing amplitude of higher harmonics in the voltage oscillations. Althought the analytical condition (25) does not depend on external flux, for parameters near the boundaries the numerical calculations show changes between both regimes; the transition to the antiphase regime starts at flux values near π.

The results obtained within the Werthamer model show also a qualitative agreement with those of the analytical treatment. Admittedly, the boundary line is shifted towards lower values of β_c. This is caused by the retarded response functions $p(t)$ and $q^0(t)$ shaming a higher effective McCumber parameter as already discussed more precisely for a single SQUID-like cell [26]. Consequently, the antiphase regime A_1 vanishes already at smaller values of $l_\parallel$ compared with the RCSJ model.

Now, we turn our attention to the phase difference ϑ within one cell. The numerical results within the Werthamer and RCSJ model are indicated in Figure 3 by symbols. Each symbol belongs to the antiphase or in-phase branch according to the respective regime between the cells. Depending on external flux this regime can vary (as discussed above) and, hence, we find jumps between the two branches within the Werthamer (Fig. 3b) and RCSJ (Fig. 3c) model. For all parameters the numerical results confirm the analytical approximations. In the Werthamer model the phase shift ϑ is slightly enhanced in comparison with the RCSJ results as it is known from the single cell. In addition, in Figures 3b and 3c for φ_e near π different solution branches (according to the in-phase or antiphase regime) are realized. This is a direct consequence from the shifted stability boundary line (*cf.* Fig. 4).

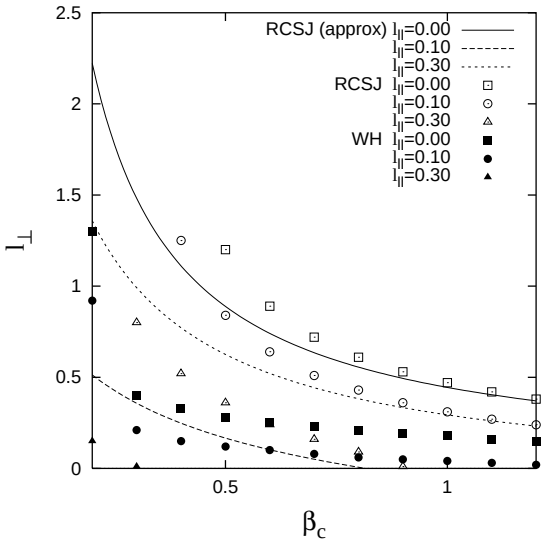

Fig. 4. Comparison of numerical results (symbols) and analytical approximation (lines) for the lower boundary between the in-phase and antiphase regime of the voltage oscillations in the two cells for $i_0 = 1.5$, $\varphi_e = 1$ and instructive values of $l_\parallel$.

5 Summary and conclusions

The phase-locking behavior of a simple two-dimensional array consisting of two connected SQUID cells is studied within the RCSJ as well as the Werthamer model. We have found a qualitative agreement between both models. Depending on the values of bias current i_0, McCumber parameter β_c and inductances $l_{\perp,\parallel}$ an in-phase or antiphase regime between the voltage oscillations of adjacent cells is obtained for a finite external flux value. The range of in-phase solutions in the Werthamer model is shifted towards lower values of β_c. In the zero-field limit for both models the locking regime is undetermined.

The phase shift between oscillations in the same cell increases with the loop inductances and the McCumber parameters of the junctions. In the Werthamer model we have found a slight enhancement of this phase shift compared with the value obtained within the RCSJ model as known from the single SQUID cell. Note that for both models in the desired in-phase regime between the cells only the inductances parallel to the current bias direction contribute to the phase shift. Therefore, assuming a small external flux one should try to make the McCumber parameters of the junctions and the inductances parallel to the current bias as small as possible, but the inductances perpendicular to the current bias has to be choosen large enough to ensure a stable in-phase regime between the cells. Note that for an extension of these results to more complex two-dimensional arrays the inductance parameters $l_{\parallel,\perp}$ should be substituted by the respective complete inductance matrix containing also mutual inductance terms.

References

1. J.B. Hansen, P.E. Lindelof, Rev. Mod. Phys. **56**, 431 (1984).
2. J.E. Lukens, in *Superconducting Devices*, edited by S.T. Ruggiero, D.A. Rudman (Academic Press, New York, 1990).
3. G. Filatrella, K. Wiesenfeld, J. Appl. Phys. **78**, 1878 (1995).
4. K. Wiesenfeld, S.P. Benz, P.A.A. Booi, J. Appl. Phys. **76**, 3835 (1994).
5. W. Yu, D. Stroud, Phys. Rev. B **46**, 14005 (1992).
6. W. Yu, K.H. Lee, D. Stroud, Phys. Rev. B **47**, 5906 (1993).
7. R. Kautz, IEEE Trans. Appl. Supercond. **5**, 2702 (1995).
8. M. Darula, P. Seidel, F. Busse, S. Benacka, Supercond. Sci. Technol. **7**, 317 (1994).
9. M. Octavio, C.B. Whan, C.J. Lobb, Appl. Phys. Lett. **60**, 766 (1992).
10. W.C. Stewart, Appl. Phys. Lett. **12**, 277 (1968).
11. D.E. McCumber, J. Appl. Phys. **39**, 3113 (1968).
12. J. Niemeyer, V. Kose, in *Superconducting Quantum Interference Devices and their Applications*, edited by H.D. Hahlbohm, H. Lübbig (Walter de Gruyter, Berlin, New York, 1977).
13. A.W. Kleinsasser, R.A. Buhrman, Appl. Phys. Lett. **37**, 841 (1980).
14. S.P. Benz, C.J. Burroughs, Supercond. Sci. Technol. **4**, 561 (1991).
15. N.R. Werthamer, Phys. Rev. **147**, 255 (1966).
16. M. Basler, W. Krech, K.Yu. Platov, Z. Phys. B **104**, 199 (1997).
17. M. Basler, W. Krech, K.Yu. Platov, J. Appl. Phys. **80**, 3598 (1996).
18. A.I. Larkin, Yu.N. Ovchinikov, Sov. Phys. JETP **51**, 1535 (1966).
19. R.E. Harris, Phys. Rev. B **10**, 84 (1974).
20. A.B. Zorin, I.O. Kulik, K.K. Likharev, J.R. Schrieffer, Fiz. Nizk. Temp. **5**, 1138 (1979).
21. A.A. Odintsov, V.K. Semenov, A.B. Zorin, IEEE Trans. Magn. **23**, 763 (1987).
22. B. Frank, H.G. Meyer, J. Appl. Phys. **72**, 2973 (1992).
23. A. Chernikov, G. Schmidt, Phys. Rev. E **52**, 3415 (1995).
24. W. Krech, Ann. Phys. (Leipzig) **39**, 117 (1982).
25. M. Basler, W. Krech, K.Yu. Platov, Phys. Rev. B **52**, 7504 (1995).
26. B. Frank, W. Krech, Phys. Stat. Sol. (b) **200**, 181 (1997).